

Reconstructed Polepieces to the Objective Magnetic Lens Depending on Some Geometrical and Physical Parameters

Wasan J. Kadhem*

Department of Applied Science, Faculty of Engineering Technology, Al-Balqa' Applied University, Amman, Jordan.

*E-mail: wasan.jawad@yahoo.com

Abstract

A function for the electron beam trajectory has been used in the present work with respect of a certain operation mode for the beams path, to synthesis the symmetrical objective magnetic lens. This function has six optimization parameters, which are respectively the action region (i.e. the air-gap), the height of electron beam trajectory, its gradient (the first derivatives) at the beginning and ending of the action region, and the length of lens. The influence of each of them is investigated concerning the objective focal properties. Indeed, the result obviously shows the effect of some of these parameters on the geometrical and physical properties to the synthesis magnetic lens, to specify the optimum symmetrical objective lens which desire, (i.e. the lens has the lowest aberration) to reconstruct its polepiece.

Keywords: Electron Optics, Synthesis, Objective Magnetic Lenses, Aberrations.

1. Introduction

Magnetic lens is defined as an axially (rotationally) symmetrical magnetic field that acts upon charged-particles beam passing through the field, which is a very similar manner to that of convex glass lenses or eye on ray of visible light passing through it. Otherwise, the essential difference between them is that magnetic (electron) lenses are concerned with continuously varying index of refraction while in glass lenses the index of refraction always change abruptly [Szilgyi 1988]. So, any axially symmetric iron-free coil represents a simplest magnetic lens, but in the modified lenses this coil surrounded by an iron circuit.

Magnetic lenses can be classified according to various criteria. The most common is the one depending on the existence of the iron circuit and the number of polepiece in that circuit. According to this criteria, magnetic lenses can be divided into four types namely, single polepiece, double polepiece, triple polepiece, and the iron-free.

When a magnetic circuit surrounds the coil, having two polepieces of ferromagnetic material, a new magnetic lens will be produced. This new design was introduced by Ruska in 1933 and usually called double polepiece magnetic lens [Riecke and Ruska 1966]. The iron core of the lens has a bore of diameter D along the axis of the coil, to allow the electrons or ions beam to pass through an air gap of width S formed in the iron circuit between the two polepieces. The magnetic field produced by energizing the coil is confined in the air gap and this causes the refractive power of the lens. Commonly the properties of this kind of lenses are expressed in terms of S/D ratio. Double polepiece lenses are said to be symmetric or asymmetric according to whether the bores in the two poles are identical or not. For more details about this kind of magnetic lenses one can see for example Liebmann [1950], Fert and Durandeu [1967], Kamminga [1976], Tsuno and Honda [1983], Juma and Yahya [1986], Britton et al [1994] and Lencova [1999].

Unfortunately magnetic lenses suffer from a number of inherent defects, called "aberrations". These aberrations can be defined as a failure of the lens system to converge the entire charged particle beam emanating from one point in the object plane into one point in the Gaussian image plane. With these defects the image will appear either blurred or distorted. Consequently, the quality of the charge particle optical devices will deteriorate.

The attempts to eliminate or at least decrease the lens aberrations have begun from the earliest days of electron and ion optics. However, some of these aberrations can be eliminated such as the asymmetries, space charge, relativistic and some of the geometrical aberrations [Grivet 1972]. While, other aberration can be corrected such as astigmatism [Grivet 1972], distortion [Hillier 1946], and anisotropic distortion [Maria and Mulvey 1977: Tsuno et al 1980: Al-Obaidi 1991: Al-Saadi 1996]. While, Scherzer has proved the impossibility of correcting both spherical and chromatic aberrations in 1936: for example see [Grivet 1972]. The failure in obtaining a free-aberrations lens led to so-called "optimization".

There are two different ways, to optimize the lens performance namely analysis and synthesis. In the first one the designer starts with actual lens design and calculates its optical properties. When the resultant properties are not electron optically acceptable, the physical and geometrical parameters of the considered design have been changed. Then the process will be repeated continuously until satisfactory values are acquired. Hence, this procedure is based on the trial and error method. In the second one, i.e. in the synthesis, one has to start with a set of performance criteria and designing an instrument to meet them [Moses 1973].

However, the synthesis procedure has a reverse process compared with its analysis counterpart. Optimization by synthesis has been given some attention during the last three decades of the last century. Since that time several different ideas had been adopted concerning the synthesis procedure, for example, the calculus of variation and intuition had been used by [Moses 1973, Trenter 1959], the optimal control procedure is followed by [Szilgyi 1977a], the dynamical programming is carried out by [Szilgyi 1977b, Szilgyi 1978] and the relatively recent approaches that use an objective or target function to start the synthesis procedure, see for example [Al-Obaidi 1995, Al-Batat 1996, Al-Jubori 2001, Al-Batat 2001, Al-Obaidi 2009].

2. The Mathematical structure of the synthesis procedure

The numerical analysis method used to accomplish this work, have been identified in three steps. In the first one the electron beam trajectory is assigned by a mathematical function or a set of data. While the second step aims to finding the axial magnetic field distribution corresponding to a certain trajectory in the first step and evaluating its objective focal properties. The final step, however, is usually concerned with obtaining the polepieces that have the ability to produce the imaging field handled in the first step.

2.1. Calculation and specified the electron trajectory

In the present work, the polynomial function of the beam trajectory along the lens axial, which has been investigated by [Kadhem and Al-Obaidi 2013] has been used but for zero operation mode. Where the axial interval of the proposed magnetic distribution is divided into three regions I, II, and III, which contain the assigned optimization parameters, see (Fig.1). The electron beam trajectory enters the lens from the left side according to zero operation mode. The optimization parameters are respectively, (1) ZS and ZF (the lens length L), (2) ZB and ZE (the action region S) where the most refractive power of the lens come from this region, (3) initial height of incident ray RS, (4) radial ray height as it enters the action region RB, (5) radial displacement of the ray as it leaves the action region RE, (6) radial height of the ray as it leaves the lens RF, (7) RBS, (8) and RES the first derivative of the ray as it enters and leaves the action region.

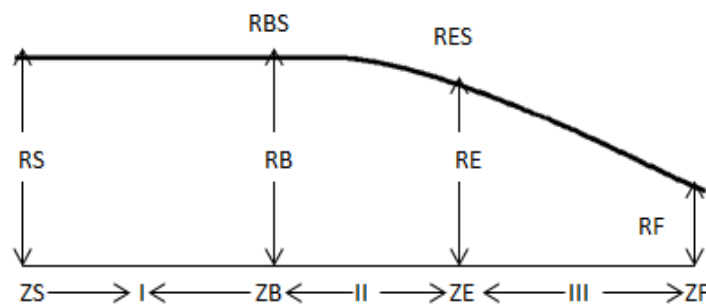


Figure 1. Electron beam trajectory for zero operation mode

2.2. Evaluation of the aberration coefficients

The spherical and chromatic aberration coefficients are the main factors that limit the resolution of objective lens. Throughout the present investigation, the spherical Cs and the chromatic Cc aberration coefficients have been calculated using the following equations: [Munro 1975].

$$C_s = (\eta/128V_r) \int_{z_o}^{z_i} \left[(3\eta/V_r) B_z^4 r_\alpha^4 + 8B_z^2 r_\alpha^4 - 8B_z^2 r_\alpha^2 r_\alpha'^2 \right] dz \quad (1)$$

$$C_c = (\eta/8V_r) \int_{z_o}^{z_i} B_z^2 r_\alpha^2 dz \quad (2)$$

Where the primes denoted to the derivative with respect to z. In objective properties, the integration covers only the interval from object plane z_o to image plane z_i in spite of the magnetic field limits. η is the electron charge-to-mass quotient and V_r is the relativistically corrected accelerating voltage. B_z is the axial magnetic flux density distribution. And r_α is the solution of the paraxial-ray equation (3), with initial condition depending on the nature of the magnetic lens operation mode:

$$r''(z) + \frac{\eta}{8V_r} B_z^2 r(z) = 0 \quad (3)$$

It should be mentioned that, throughout the present work the cubic spline differentiation technique and function.

2.3. Calculation of the polepiece profile

The polepiece profile that can generate the optimum field (the field have the lowest aberrations) must be determine. In fact, when the cubic splin expression of the potential is used in Laplace's equation, all terms will be vanishes except the first two terms. Therefore, the following equipotential surface equation can be obtained [Szilagyí 1984]:

$$R_p(z) = 2 \left[(V_z - V_p) / V_z'' \right]^{1/2} \quad (4)$$

Where $R_p(z)$ is the radial height of the equipotential surface along the optical axis, V_z is the axial magnetic scalar potential distribution, V_z'' is the second derivative of V_z and V_p is potential at the equipotential surface. Thus the V_z distribution corresponding to the optimum field must be calculated firstly in order to obtain the polepiece configuration. Thus, this is the topic of the next paragraph.

2.4. Determination of the magnetic scalar potential

The cubic spline integration technique which has been introduced by Al-Obaidi [1995], is used to obtained the magnetic scalar potential. According to this method, the optical axis z is divided into (n-1) subintervals, where n is the number of the (z, B_z) points. The axial magnetic flux density distribution B_z for each subinterval is represented by the following cubic spline expression:

$$B_z(z) = B_j + B'_j(z - z_j) + 0.5B''_j(z - z_j)^2 + \frac{B''_{j+1} - B''_j}{6(z_{j+1} - z_j)}(z - z_j)^3 \quad (5)$$

Where $z_j \leq z \leq z_{j+1}$ and $j = 1, 2, 3, \dots, (n-1)$. The following equation:

$$B_z = -\mu_o \frac{dV_z}{dz} \quad (6)$$

Now, by substituting equation (5) in equation (6) and integrating over each subinterval (j), the following recurrence formula will be obtained;

$$V_{z(j+1)} = V_{zj} - E_j \quad (7)$$

Where $V_{z(j+1)}$, V_{zj} are the magnetic scalar potential at the terminals of the subinterval (j) and E_j is a cubic expression having the forms;

$$E_j = \left[V'_j h_j + V''_j \left(\frac{h_j^2}{2} \right) + \left(V'''_j + \frac{V'''_{j+1}}{3} \right) \left(\frac{h_j}{2} \right)^3 \right]$$

Where h_j is the width of the subinterval (j).

For symmetrical imaging field distributions, one can put;

$$V_{zn} = -V_{z1} = 0.5 NI \quad (8)$$

Where V_{zn} , V_{z1} are the potential at the terminal points of the optical axis ZF and ZS respectively and NI is the

area under B_z distribution curve (i.e. the lens excitation). Hence, the recurrence formula (7) can be written in the following form;

$$V_{z(j+1)} = 0.5 \sum_{i=1}^{n-1} E_i - \sum_{j=1}^{j=i} E_j \quad (9)$$

For each subinterval $z_j \leq z \leq z_{j+1}$. Therefore, one can obtain the symmetrical magnetic scalar potential along the lens interval.

3. Results and Discussion

The influence of varying of the previous optimization parameters on the optical properties of the objective lens and hence the reconstruct pole pieces has been carried out when the $NI/\sqrt{V_r} = 20$, at which the objective lenses operate usually, [Hawkes 1982].

It should be mentioned that, because of the inflexibility of the function used in the present work, may be faced difficulty in controlling all the parameters at a fixed values during a study one of them. Anyhow, the effect of the action region has been investigated at the values of $S = 2.2, 4, 6, 8$, and 10 (in unit of millimeter), the remaining parameters are kept fixed at $L=42$ mm, $RS=1000$ mm, $RB=999.99999$ mm, $RE=980$ mm, and $RBS=0$. While, the parameter RES is left to change randomly with S . (Table 1) and (Fig.2) shows some of the magnetic field parameters and the optical properties respectively, for the deduced imaging fields as a function of the optimization parameter S .

Table 1. Conventional parameters of lenses for the deduced fields versus the parameters S at $NI/\sqrt{V_r} = 20$.

S(mm)	D(mm)	S/D	$B_{max}(T)$	W(mm)	NI(A.t)	RES
2.2	0.08	27.5	0.1676	1.89	227.42	-18.12
4	0.10	40	0.0923	3.466	230.75	-9.96
6	0.12	50	0.0615	5.210	230.80	-6.63
8	0.14	57	0.0461	6.950	230.77	-4.97
10	0.16	63	0.0369	8.687	230.81	-3.97

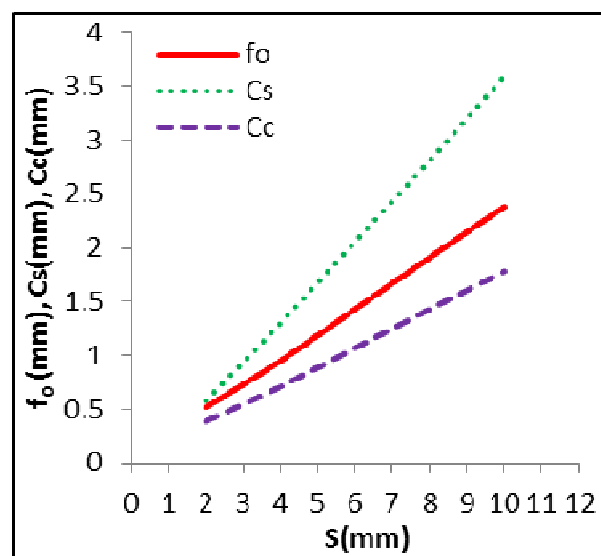


Figure 2. The aberration coefficients C_s , and C_c and the objective focal length as a function of the parameter S .

Obviously, the results are denote to strong significance influence on the imaging field properties is inherent as long as S varied. However, this behavior may thought as a consequence to the increases in the lens (imaging field) power due to the decreases in the action region, see (Fig.3).

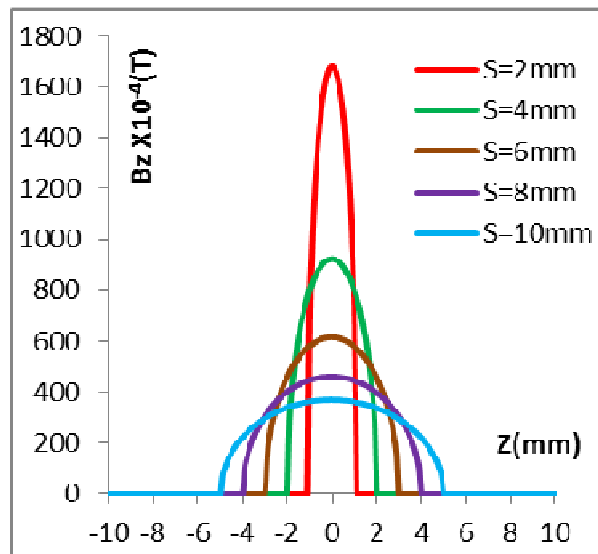


Figure 3. The magnetic field distribution B_z along the optical axis of lens at various values of the parameters S .

The corresponding magnetic scalar potential of B_z distribution plots in (Fig.3), is shown in (Fig.4). Furthermore, the pole piece profiles that can produce each B_z distribution in (Fig.4) is plotted in (Fig.5), it can be seen that, the consequences for increasing in S lead to decreasing in the pole-face curvature and hence the pole diameter D , see (Table 1).

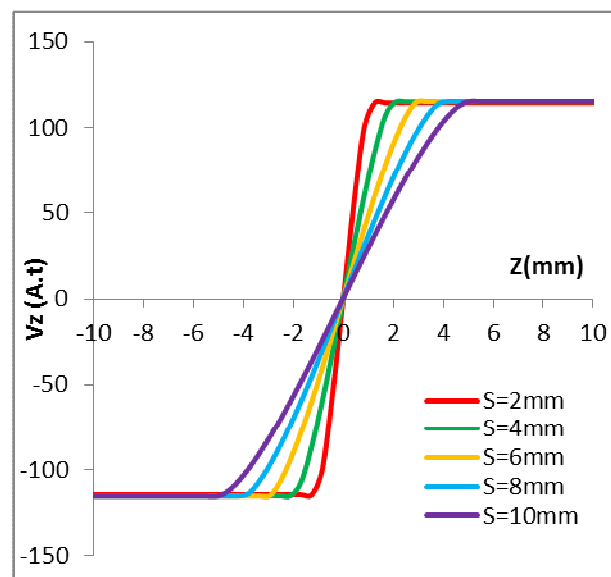


Figure 4. The V_z distribution along at various values of S .

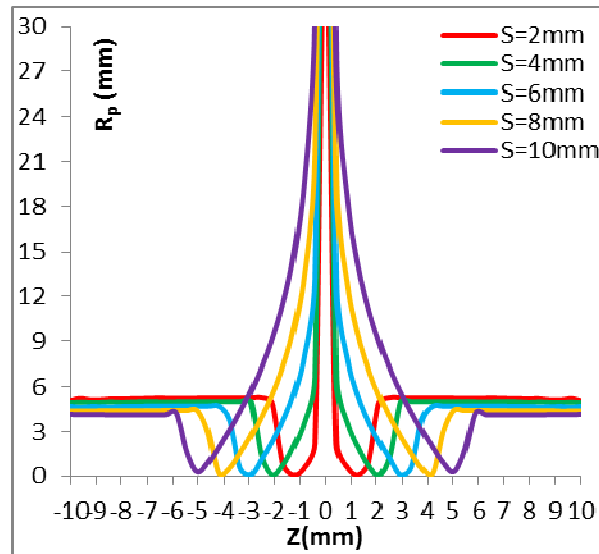


Figure 5. The reconstructed pole pieces shapes at various values of S.

In order to implement the calculation of lens length L, five values of this parameter were chosen at (22, 42, 62, 82, and 102) mm, see (Table 2). When the remaining parameters are kept constant at the following values S=2.2mm, RS=1000mm, RB=999.99999mm, RE=980mm, and RES=RBS=-18.12. However, Table 2 shows several conventional parameters at various values of L. It can be seen that the parameter L does not affect the properties of the resultant imaging field. Actually, this is an expected result, since the refractive power is approximately confined only in the action region.

Table 2. Conventional parameters of lenses at various values of L at $NI/\sqrt{V_r}=20$

L (mm)	D (mm)	f_0 (mm)	Cs (mm)	Cc (mm)	B_{max} (T)	W (mm)	NI (A.t)
from 22 to 102	0.08	0.52	0.58	0.39	0.1676	1.89	227.42

Regarding the RB parameter. Unfortunately this parameter cannot be studied individual, because two parameters (RES and RBS) must be varied whenever RB is change. All parameters values are remained fixed at the same values of the previous paragraph, while RB is varied. However, the decreases in RB associated with the decreasing of |RES| and increasing of |RBS|, this must be done so as to meet such a variation as shown in (Table 3) and (Fig.6). It is clear that for this case the aberrations get rise better as long as RB increased. The axial magnetic field distribution for each value of RB and the corresponding reconstructed polepiece shapes capable to produce these distributions are plotted in (Fig.7) and (Fig.8), respectively. This figures indicates that, at RB=1000mm the bore diameter D of the pole is more large from that of other bores and the air-gap is changed to be 2.6mm instead of 2.2mm. This because of the value of RBS=0.

Table 3. Conventional parameters of lenses at various values of RB at $NI/\sqrt{V_r}=20$.

RB(mm)	D(mm)	S/D	B_{max} (T)	W(mm)	NI(A.t)	RBS	RES
1000	0.16	13.75	0.168	1.897	237.42	0	-18.12
999	1.4	1.57	0.162	1.898	234.38	-0.15	-17.22
998	1.5	1.46	0.156	1.900	232.08	-0.30	-16.01
997	1.6	1.37	0.150	1.901	228.09	-0.45	-14.96
996	1.7	1.29	0.144	1.903	223.05	-0.60	-13.90

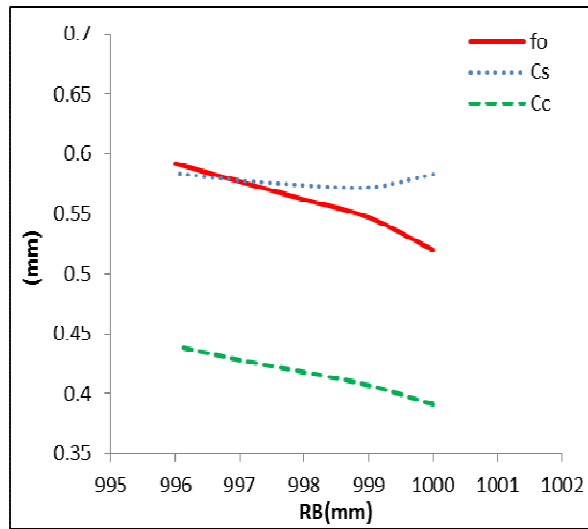


Figure 6. The aberration coefficients C_s , and C_c and the objective focal length as a function of the parameter RB .

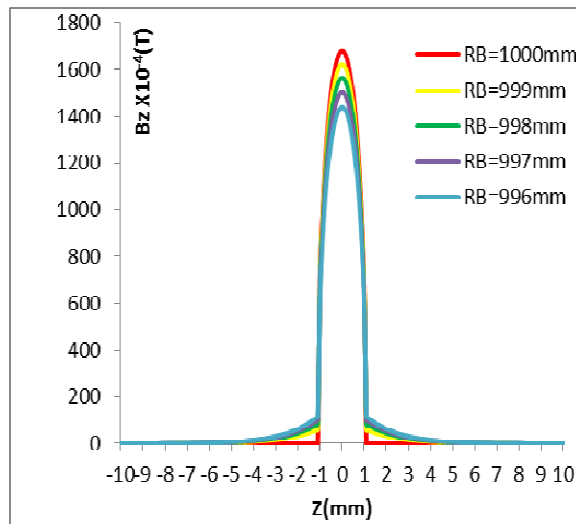


Figure 7. The magnetic field distribution B_z along the optical axis of lens at various values of the parameters RB .

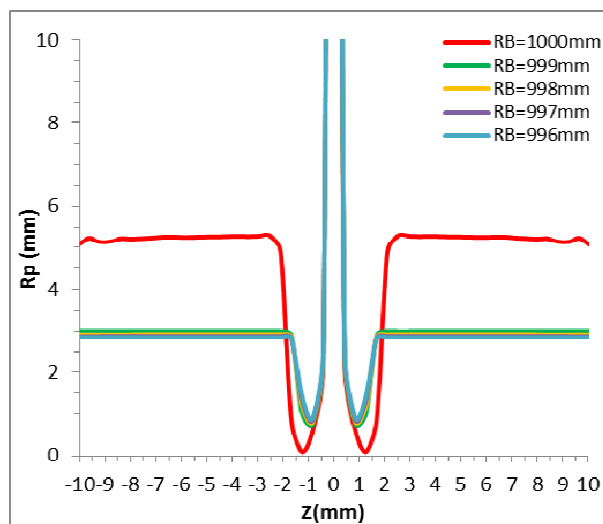


Figure 8. The reconstructed pole pieces shapes at various values of RB .

Concerning with the parameter RE the following values: 950,960,970, 980, and 990mm has chosen to clarify their influence on the imaging field objective properties, where the remaining parameters are kept constant at this values: S=2.2mm, L=42 mm, RS=1000mm, RB=999.99999mm, and RES=RBS. Consequently, as long as RE varied the correspondence gradient needs to be varied too as shown in (Table 4). In fact, the scientific reason behind this bullying variation is that the trajectory is forced to meet null magnetic field at the terminal point ZF. So, when RE increased it is necessary to decrease |RES| so as to achieve such a requirement. Actually, this parameter in not effected on the objective properties, but the excitation, the maximum magnetic field and the gradient of the trajectory at the terminal point ZE decreases when RE is decreased.

Table 4. Conventional parameters of lenses at various values of RE at $NI/\sqrt{V_r}=20$

RE (mm)	f_o (mm)	Cs (mm)	Cc (mm)	B_{max} (T)	W (mm)	NI (A.t)	RES
990	0.520	0.583	0.391	0.118	1.896	160.69	-9.07
980	0.520	0.583	0.391	0.167	1.897	227.24	-18.12
970	0.520	0.584	0.391	0.205	1.898	278.75	-27.16
960	0.520	0.585	0.391	0.237	1.899	322.14	-36.17
950	0.520	0.585	0.391	0.265	1.899	360.46	-45.17

The parameter RES is analyzed for the arbitrary values listed in (Table 5), when the other parameters are fixed at the same values quoted above. Unfortunately, the values of RES which investigated are the only set that leads to obtain imaging fields, so variation of the properties may seem to be insignificant. In the other side, one can realize that decreases of RES values improved the quality of the imaging field.

Table 5. Conventional parameters of lenses at various values of RES at $NI/\sqrt{V_r}=20$

RES	f_o (mm)	Cs (mm)	Cc (mm)	B_{max} (T)	W (mm)	NI (A.t)
-18.126	0.520	0.583	0.391	0.1676	1.897	227.42
-18.134	0.520	0.583	0.391	0.1677	1.897	227.47
-18.142	0.520	0.583	0.391	0.1678	1.896	227.52
-18.150	0.520	0.583	0.391	0.1679	1.895	227.57
-18.158	0.521	0.584	0.392	0.1680	1.894	227.62

Unluckily, we could not study variable RBS individually. But its influence can be seen on the focal properties of the lens during study variable RB, as shown above in (Table 3). Furthermore, it is obvious that as long as RB increased, RBS is decreased and this leads to improvement in the objective properties of lens. It is the opposite of the behavior of the variable RES and its impact on the properties, see (Fig.9).

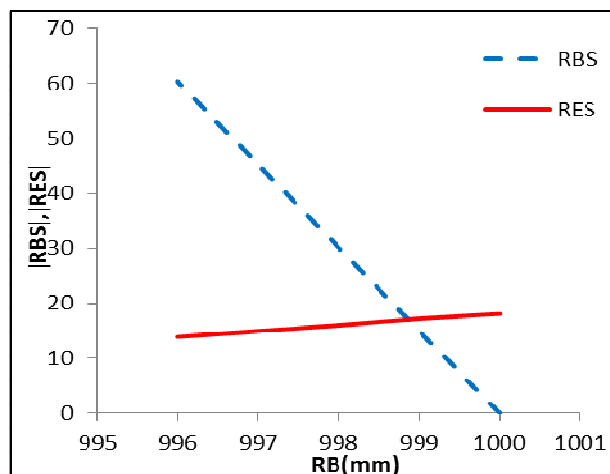


Figure 9. The variation of the parameter RBS and RES with the parameter RB.

As a result, one can remark from the information quoted in the above tables the optimum magnetic field distribution and the correspondence polepieces profile, that could produce for the trajectory assigned by the following parameters $S=2.2\text{mm}$, $L=42\text{mm}$, $RS=1000\text{mm}$, $RB=999.9999\text{mm}$, $RE=980\text{mm}$, $RBS=0$, and $RES=RES=-18.1$.

4. Conclusion

It is apparent from the present work that the polynomial function can be used to synthesize the symmetrical and asymmetrical objective double polepiece lenses operated with low excitation (unsaturated). The deduced conventional reconstructed polepieces shapes, have a lower aberrations compared with the same physical and geometrical parameters. So, it is necessary to put such a designs into reality by designers and manufactures.

References

- Al-Batat, A.H. (1996), "Inverse design of magnetic lenses using a new magnetic field", *M.Sc. Thesis*, Al-Mustansiryah University, Baghdad, Iraq.
- Al-Batat, A.H. (2001), "A theoretical and computational investigation on magnetic lenses synthesis", *Ph.D. Thesis*, Al-Mustansiryah University, Baghdad, Iraq.
- Al-Jubori, W. J. (2001), "Inverse design of asymmetrical magnetic lenses in the absence of magnetic saturation", *Ph.D. Thesis*, Al-Mustansiryah University, Baghdad, Iraq.
- Al-Obaidi, H. N. (1991). "Design of electromagnetic lenses", *M. Sc. Thesis*, University of Al-Mustansiryah, Baghdad, Iraq. (In Arabic).
- Al-Obaidi, H.N. (1995), "Determination of the design of magnetic electron lenses operated under preassigned magnification conditions", *Ph.D. Thesis*, Baghdad University, Baghdad, Iraq.
- Al-Obaidi, H.N., Mahdi, A.S. & Kadhem, W. J. (2009) ," Failure limit investigation for the spline aided solution technique", *J. Mod. Phys. Lett. B* 23 (11) 1467–1477.
- Al-Saadi, A. K. (1996), "Computations on the properties of magnetic doublet lenses for the transmission electron microscope", *Ph.D. Thesis*, University of Al-Mustansiryah, Baghdad, Iraq.
- Britton, D. T., Uhlmann, K. & Kogel, G. (1994), "Magnetic positron optics", *Appl. Surf. Sci.*, 85, 158-164.
- Fert, G. and Durandea, P. (1967), "Magnetic electron lenses". *Focusing of charged particles*, 1ed. A. Septier. (New York: Academic), 309-352.
- Grivet, P. (1972), "Electron optics", 2nd Ed. *Pergamon press*.
- Hawkes, P. W. (1982), "Magnetic electron lenses", *Springer-verlag*.
- Hillier, J. (1946), "A study of distortion in electron microscope projection lenses", *J. Appl. Phys.* 17. 411-419.

- Juma, S. M., Yahya, A. A. (1986), "Focal properties of unsaturated asymmetrical magnetic electron lenses". *J. Phys. E: Sci. Instrum.* 19, 614-624.
- Kadhem, W. J. & Al-Obaidi, H. N. (2013), "An inverse design approach for magnetic lenses operated under infinite magnification condition", *Optik* 124, 3523-3526.
- Kammaing, W. (1976), "Properties of magnetic objective lenses with highly saturated polepieces". *Optik*, 45, 39-54.
- Lencova, B. (1999), "Accurate computation of magnetic lenses with FOFEM", *Nucl. Inst. And Meth. Phys. Res. A*, 427, 329-337.
- Liebmann, G. (1950), "Field plotting and ray tracing in electron optics, (A review of numerical methods)", *Adv. Electron*, 2ed., L. Marton, (Academic press: New York), 101-149.
- Maria, F. Z. & Mulvey, T. (1977), "Scherer's formulae and the correction of spiral distortion in the electron microscope". *Ultramicroscopy*, 2, 178-192.
- Moses, R.W. (1973), "Lens optimization by direct application of the calculus of variation":, *Image Processing and Computer Aided Design in Electron Optics*, Hawkes, P.W. (Eds.) *Academic Press*, 250-272.
- Munro, E. (1975), "A set of computer programs for calculating the properties of electron lenses", University of Cambridge, department of engineering *report CUED/B-Elect. TR 45*.
- Riecke, W. D. & Ruska, E. (1966), "A 100 KV Transmission Electron Microscope With Single-Field Condenser Objective Electron Microscopy", 1ed. R. Uyeda (Tokyo: Maruzen), 19-20.
- Szilagy, M. (1977a), "A new approach to electron optical optimization", *Optik* 48, 215-224.
- Szilagy, M. (1977b), "A dynamic programming search for magnetic field distribution", *Optik* 49, 223-246.
- Szilagy, M. (1978), "A dynamic programming search for electrostatic immersion lenses with minimum spherical aberration", *Optik* 50 35-57.
- Szilagy, M. (1984), "Reconstruction of electrode and polepiece from optimized axial field distortion of electron and ion optical system", *Appl. Phys. Lett.* 45, 499-501.
- Szilagy, M. (1988), "Electron and ion optics", *plenum press*: New York.
- Trenter, W. (1959), "Existenzbereiche Rotations Symmetrischer Elektronenlinsen (Limits on the properties of rotationally electron lenses)", *Optik* 16 155-184.
- Tsuno, K., Arai, Y. & Harada, Y. (1980), "Elimination of spiral distortion in electron microscopy by means of three-pole-piece lens". *Elec. Micr.*, 1, 76-77.
- Tsuno, K., & Honda, T. (1983), "Magnetic field distribution and optical properties of asymmetrical objective lenses for an atomic resolution high voltage electron microscope". *Optik*, 64, 367-78.